Author Manuscript

Author Manuscript

Author Manuscript

Author Manuscript

HHS Public Access

Author manuscript

*Environ Sci Process Impacts*. Author manuscript; available in PMC 2016 January 11.

Published in final edited form as:

*Environ Sci Process Impacts*. 2013 June ; 15(6): 1191–1198. doi:10.1039/c3em00108c.

# Comparison of field portable measurements of ultrafine $TiO_2$: X-ray fluorescence, laser-induced breakdown spectroscopy, and Fourier-transform infrared spectroscopy

**Ryan F. LeBouf**[a], **Arthur L. Miller**[b], **Christopher Stipe**[c], **Jonathan Brown**[c], **Nate Murphy**[b], and **Aleksandr B. Stefaniak**[a]

Ryan F. LeBouf: rlebouf@cdc.gov

[a]Division of Respiratory Disease Studies, National Institute for Occupational Safety and Health, Morgantown, WV, 26505 USA

[b]Office of Mine Safety and Health Research, National Institute for Occupational Safety and Health, Spokane, WA 99207, USA

[c]Department of Mechanical Engineering, Seattle University, Seattle, WA 98122, USA

## Abstract

Laboratory measurements of ultrafin0e titanium dioxide ($TiO_2$) particulate matter loaded on filters were made using three field portable methods (X-ray fluorescence (XRF), laser-induced breakdown spectroscopy (LIBS), and Fourier-transform infrared (FTIR) spectroscopy) to assess their potential for determining end-of-shift exposure. Ultrafine $TiO_2$ particles were aerosolized and collected onto 37 mm polycarbonate track-etched (PCTE) filters in the range of 3 to 578 μg titanium (Ti). Limit of detection (LOD), limit of quantification (LOQ), and calibration fit were determined for each measurement method. The LOD's were 11.8, 0.032, and 108 μg Ti per filter, for XRF, LIBS, and FTIR, respectively and the LOQ's were 39.2, 0.11, and 361 μg Ti per filter, respectively. The XRF calibration curve was linear over the widest dynamic range, up to the maximum loading tested (578 μg Ti per filter). LIBS was more sensitive but, due to the sample preparation method, the highest loaded filter measurable was 252 μg Ti per filter. XRF and LIBS had good predictability measured by regressing the predicted mass to the gravimetric mass on the filter. XRF and LIBS produced overestimations of 4% and 2%, respectively, with coefficients of determination ($R^2$) of 0.995 and 0.998. FTIR measurements were less dependable due to interference from the PCTE filter media and overestimated mass by 2% with an $R^2$ of 0.831.

## Introduction

In animal studies, inhalation of ultrafine (<100 nm) titanium dioxide ($TiO_2$) particles has been associated with greater pulmonary inflammation than its fine (<2.5 μm) counterpart on a similar mass-basis.[1,2] The National Institute for Occupational Safety and Health currently recommends a mass-based exposure limit (respirable) of 2.4 mg $m^{-3}$ for fine $TiO_2$ and 0.3 mg $m^{-3}$ for ultrafine $TiO_2$ because particle number and surface area of the latter aerosol is

Correspondence to: Ryan F. LeBouf, rlebouf@cdc.gov.

Author Manuscript Author Manuscript Author Manuscript Author Manuscript

significantly higher.[3] The American Conference of Governmental Industrial Hygienists recommends a threshold limit value of 10 mg $m^{-3}$ (total dust), but does not distinguish between ultrafine and fine homologues.[4] A cohort mortality study among fine titanium dioxide manufacturing workers in the United States revealed $TiO_2$ total dust exposures of 6.2 ± 9.4 mg $m^{-3}$ ($n$ = 686) among workers in the job category "packers, microionizers, and addbacks".[5] The data also revealed that exposures had been decreasing between 1976 and 2000. In a recent field study of metal oxide nanoparticle exposures in the workplace, handling tasks (including collecting, weighing, and transferring powders) produced the highest geometric mean personal exposures to respirable $TiO_2$ at 53.14 μg $m^{-3}$ ($n$ = 5).[6] While the exposure was 17% of the NIOSH REL, it is common to characterize a sampling and analytical methodology at or below 10% of the occupational exposure limit to capture these lower-exposure events. Current exposure assessment approaches involve real-time instrumentation such as particle counting which suffers from a lack of specificity, or integrated filter-based sampling techniques. The latter require laboratory-based gravimetric or atomic spectrometry techniques to determine mass; these techniques also involve shipping and handling procedures that may affect sample integrity prior to receipt by the analytical laboratory, lag times of several days between collection and analysis, and/or sample preparation protocols involving acid digestion prior to analysis.

Exposure to nanoscale titanium dioxide particles during production or use may occur quickly and the titanium-bearing aerosol may not be in a pure state. Particle concentrations are influenced by auxiliary processes such as diesel forklift exhaust and external factors such as outdoor sources.[7] For example, Koivisto *et al*. (2012) evaluated exposures among workers engaged in packaging ultrafine $TiO_2$ using non-specific real-time aerosol monitors augmented by particle collection onto grids with subsequent analysis using transmission electron microscopy (TEM).[8] The authors noted confounding of real-time measurements from auxiliary sources (*e.g.*, soot and process chemical emissions). Additionally, results of expensive and time-consuming TEM analysis of grid samples identified soot and sulfur-containing particles among $TiO_2$ particles. Hence, a need exists for rapid and selective characterization of nanoscale titanium mass content in workplace atmospheres. Field techniques such as portable X-ray fluorescence (XRF), laser-induced breakdown spectroscopy (LIBS) and Fourier-transform infrared (FTIR) spectroscopy may provide expedient, specific characterization of sampled mass at the end of a work shift to provide daily feedback of mass-based metal exposures. Since XRF and FTIR techniques are non-destructive and sample integrity is retained, the sample may be subsequently analyzed to gain additional insights on exposure characteristics, *e.g.*, electron microscopy (particle morphology), gas adsorption (surface area), or confirmation of mass (atomic spectroscopy).

The overall goal of this project was to evaluate the efficacy of portable XRF, LIBS, and FTIR instruments to reliably measure Ti content on filter media containing ultrafine $TiO_2$. This research was the first step in identifying selective quantitation methods for analyzing titanium content of mixed aerosols. The specific aims were to:

1. Evaluate instrument detection limits, quantification limits, and calibration characteristics using filter samples with known $TiO_2$ masses;

Author Manuscript Author Manuscript Author Manuscript Author Manuscript

2. Establish the linear dynamic range of each instrument and develop an algorithm for conversion of instrument response to $TiO_2$ mass loadings on filters.

## Materials and methods

### Sample collection

Ultrafine $TiO_2$ powder, Degussa P25, was chosen for this study. It consists of a combination of anatase and rutile primary particles of mean diameter 20 nm that form agglomerates of mean diameter 67 nm. It was aerosolized in a well-characterized inhalation chamber at a nominal 6 mg $m^{-3}$ concentration for all phases of the research.[9] Particle samples were collected on 37 mm polycarbonate track etched (PCTE) filters having 0.4 μm pore size (Sterlitech Corporation, Kent, WA), as previously used in a surface area study of $TiO_2$, using two-piece, closed-face cassettes attached to GilAir-5 air sampling pumps (Sensidyne, Clearwater, FL) operated at 3 LPM.[10] Closed-face cassettes produce a non-uniform deposition pattern with heavier loadings on the filter below the inlet orifice,[11] especially when sampling at this relatively high flow rate. This heterogeneous deposition pattern must be considered when analyzing the filter mass loadings using techniques that only interrogate a portion of the filter.

The $TiO_2$ mass loading on filters was determined gravimetrically with three measurements per filter using a calibrated microbalance (Mettler-Toledo) and passed through a U-shaped static charge neutralizer (Haug GMBH + Co. KG, Germany) after temperature- and humidity-controlled equilibration for 24 hours prior to weighing. The mass of Ti was calculated from the gravimetric $TiO_2$ mass value using a conversion factor of 0.599 (atomic mass of Ti divided by the molecular weight of $TiO_2$). Portable XRF, FTIR and LIBS measurements were used to determine Ti content for each filter sample. A total of 72 samples were collected at masses ranging from 3 to 578 μg Ti (Table 1). Most samples (#13–28, 30–72) were analyzed by XRF; only a subset of samples were analyzed by LIBS (#1, 3, 5, 8, 17, 18, 36, 41, 50, 55, 56, 59, 63, and 66) and FTIR (#2, 25, 34, 37–42, 44–50, 52–56, 58–60, 62–72).

### XRF

In this technique, absorption of X-rays leads to excitation of atoms in the sample with subsequent relaxation from (excited) higher energy states to the ground state, which occurs *via* electronic transitions that are characterized by the release of x-radiation (or fluorescence). The energy or wavelength of this fluorescence is unique for most atomic transitions and at a longer wavelength than the absorption edge.[12] The intensity of fluorescence is proportional to the mass of the material excited.

Titanium has an atomic number of 22 and produces K-series fluorescence emissions regardless of the physical or chemical state of the element since the electrons responsible for fluorescence take no part in bonding.[12] This is worth noting since the instrument in this study was calibrated to pure Ti but used to measure $TiO_2$. A caveat of XRF for the determination of elements below atomic number 23 is Auger electron emission, a competing

Author Manuscript Author Manuscript Author Manuscript Author Manuscript

process, which reduces fluorescence intensity to a greater extent as the atomic number decreases.[12]

The XRF instrument used for this study was a Portable Vacuum Alloy Analyzer (Alpha-8000LZX; Olympus INNOV-X, Woburn, MA) with a 1 $cm^2$ analysis window and an XT-220 X-ray tube at 35 kV and 20 μA. Detector counts were recorded at 4.5 eV; measurements were recorded in units of μg Ti per $cm^2$ using the internal instrument algorithm for converting detector counts to mass loading for titanium (*i.e.* factory calibration). Elemental titanium standards mounted on a 6.3 μm Mylar polyester film (Micromatter, Vancouver, BC) in the range 25.1 to 134.1 μg $cm^{-2}$ were measured to check the factory calibration.

The overall analysis strategy included collecting multiple measurements across the face of the 37 mm filter to account for heterogeneous particle deposition with the intent of incorporating the measurements into an algorithm for estimating a single value of total mass loading. To collect multiple measurements among sites on the filter, a holder was constructed to fix the circular analysis window (diameter = 4.75 mm) over five points on the filter: center (C), top (T), bottom (B), left (L), and right (R).

Statistical analyses including distribution tests for normality and orthogonal regression were performed in JMP (SAS Institute Inc., Cary, NC). Statistically significant differences among filter measurement positions were investigated using comparisons of group means ($\alpha$ = 0.05).

In order to integrate the readings into a total filter loading (μg per filter), a multiple linear regression with no intercept[11] was performed in SAS (SAS Institute Inc., Cary, NC) using the gravimetric mass of the samples and the Ti readings at each measurement position. The raw instrument readings in μg $cm^{-2}$ were regressed against the gravimetric mass in μg per filter. No correction for the surface area analyzed was necessary since the regression develops a predictive relationship between the instrument readings and the gravimetric mass. Best fit coefficients were determined for a five- and two-point reading model according to the following equations:

$$\text{Gravimetric mass} = \alpha_1 C + \alpha_2 T + \alpha_3 B + \alpha_4 R + \alpha_5 L$$

and

$$\text{Gravimetric mass} = \beta_1 C + \beta_2 T$$

where $\alpha_1$ to $\alpha_5$ = coefficients for the five point model; $\beta_1$ and $\beta_2$ = coefficients for the two-point model; and C, T, B, R, and L = center, top, bottom, right, and left measurements, respectively. Results from the two model types were then compared to the gravimetric results using percentage recovery (% recovery = predicted mass/gravimetric mass × 100%) in order to determine the most appropriate model.

Author Manuscript Author Manuscript Author Manuscript Author Manuscript

## LIBS

LIBS technique uses a focused, pulsed laser beam to vaporize material from and generate a plasma on the surface of a sample.[13] As the plasma cools and continuum (Bremsstrahlung) emission from the plasma fades, longer-lived fluorescence from neutral and ionized species is observed and used to identify and quantify atomic composition. The advantages of LIBS include minimal sample preparation, rapid analysis, ability to measure light elements, and the simultaneous detection of multiple elements that emit light from the UV to the near IR, making it well suited to commercial applications in the areas of geology, metallurgy, forensics, and industrial quality control.

A number of previous studies report LIBS measurements of particulate matter deposited on filters. Cremers and Radziemski measured beryllium deposited on filters with detection limits ranging from 0.012 to 0.450 μg $cm^{-2}$.[14] Neuhauser *et al*. detected 12 types of metal particles on glass microfiber filters with detection limits ranging from 0.01 to 0.44 μg $cm^{-2}$.[15] Panne *et al*. collected and detected heavy metal particles on quartz fiber filters.[16] Self-absorption was observed above mass loadings of 50 to 100 μg $cm^{-2}$. SEM images showed that the laser pulse did not fully penetrate the filter when using a 532 nm laser pulse with energy of approximately 30 mJ and a typical spot size of 220 μm. The authors report that for mass loadings below 10 μg $cm^{-2}$ a majority of the aerosol mass is ablated in a single pulse, and detection limits were reported from 0.01 to 0.91 μg $cm^{-2}$.

The LIBS system used for this study was an Insight™ (TSI Inc., Redmond, WA). The system employs a 1064 nm Nd:YAG laser emitting 50 mJ, 7 ns pulses to a spot size at the filter surface of 400 μm. Emitted light from the plasma is collected in a bundled fiber optic cable and routed into a 0.3 m Czerny-Turner style spectrometer with an iCCD camera, resulting in a spectral resolution of approximately 0.2 nm. A spectrometer delay time of 2 μs and a gate of 1 μs were used.

For LIBS measurements, each filter was cut into 10 pieces, and each piece was analyzed separately with a single laser shot. To prepare the 10 pieces, the edge of each 37 mm circular filter was pinned onto a dense cardboard sheet and cut into a grid pattern, resulting in square pieces roughly 7 mm × 7 mm. This approach allowed for multiple measurements of the same sample to average out both shot-to-shot noise and variation in deposition across the filter. In addition, it eliminated a measurement artifact seen when making multiple measurements on a single uncut filter where the pressure induced shockwave disperses and deposits material elsewhere on the filter making subsequent shots on the sample filter inaccurate.[17] As shown in Table 1, fourteen samples, spanning the range 3 to 252 μg Ti per filter, were analyzed by LIBS. Titanium spectral emission lines at 264.6 and 336.1 nm were integrated as a measure of titanium abundance.

## FTIR

FTIR spectrometry entails illumination of the sample with multi-wavelength radiation using an IR emitting source and an interferometer. The IR beam interacts with the sample, which absorbs part of the radiation, and the return signal is collected by a detector and analyzed using a Fourier transform algorithm, generating an “absorbance spectrum”.[18] The

Author Manuscript Author Manuscript Author Manuscript Author Manuscript

absorbance spectrum shows which wavelengths have been absorbed by unique molecular bonds in the sample, and can thus be used to identify and quantify compounds containing those bonds. Unlike XRF and LIBS, FTIR is therefore used to quantify the molecule $TiO_2$, as opposed to elemental Ti.

FTIR is especially well suited to identification of materials that have molecular bonds that absorb at specific wavelengths. Absorption requires that molecules have a permanent dipole moment and vibrate about a bond, changing the bond length or angle, or rotate about an axis perpendicular to the bond.[19] This excludes diatomic molecules like nitrogen but includes many other bonds which allow FTIR studies of many materials including the capturing of bond transitions during chemical reactions.[20] Application of FTIR to quantification of mineral dusts on filter samples has been previously demonstrated.[21,22] Mass of silica ($SiO_2$) deposited on filter material was accurately quantified using spectral background subtraction to remove the contribution of the filter material from the FTIR spectrum.[21]

The FTIR spectrometer chosen for this study (Model Alpha, Bruker Optics, Billerica, MA) was designed for field portability and has the potential sensitivity to quantify small amounts of $TiO_2$ dust deposited on filters. For this study, the resolution was set to 4 $cm^{-1}$, which has been shown previously to eliminate unnecessary detail and thereby reduce noise while still providing adequate peak identification and maintaining a reasonably quick sampling time.[23]

Each sample underwent a sequence of 40 scans (determined by experimentation to produce adequate signal to noise ratio), and a combined absorbance spectrum was generated and saved for analysis. Integration of the baseline-corrected absorbance spectrum between 800 and 470 $cm^{-1}$ was used as a measure of the mass of $TiO_2$ in each sample. Because anatase and rutile forms of $TiO_2$ have broad absorbance peaks in this range[20,24] and since the $TiO_2$ used in this study is an 80/20 mixture of anatase and rutile, it was necessary to use a broad integration range, and the resulting quantitation is not specific to either form but rather a combination of the two.

FTIR analyses of $TiO_2$ were conducted using three different modes: transmission, diffuse reflectance (DR) and attenuated total reflection (ATR).[18] All three methods were briefly evaluated and based on the preliminary data, the transmission method was chosen for comparison with other spectrometry methods, due to its better performance on the filter samples.

To analyze filter samples with the FTIR instrument in transmission mode, the filter was mounted in a stainless steel holder that was placed so that the filter was centered between the horizontal IR source beam and the detector, where the beam is at its narrowest diameter of 6 mm. All samples were analyzed once in the center, as was done in a previous related study.[21]

It was noted that the absorbance of the blank filter was intense (above three absorbance units), and that this extreme absorption interfered with analysis of the $TiO_2$ peak when background was subtracted from the spectrum. Therefore, a blank filter was included in the sample set and assigned a value of 0 μg $TiO_2$.

Author Manuscript Author Manuscript Author Manuscript Author Manuscript

The FTIR instrument was calibrated empirically by correlating the integrated spectral data with the gravimetrically determined mass of $TiO_2$ for a subset of the samples. The regression equations derived from the calibration curves were then used to predict the mass of $TiO_2$ on a separate set of unknown samples using the raw FTIR data.

## Results and discussion

### XRF

An initial limit of detection (LOD) of 22.4 μg Ti per filter was estimated based on three standard deviations above the mean blank filter signal ($n = 3$). The estimated limit of quantification (LOQ), calculated as 3.33 × LOD, was 74.5 μg Ti per filter. The estimated LOD and LOQ are comparable to calculated values using mixed cellulose ester filters in a recent thesis.[25] The LOQ was used to parse the data into a reasonable mass loading range for calculating the LOD based on a regression that included a range of values below the estimated LOD to the estimated LOQ. The actual LOD was calculated as the standard error of the regression multiplied by three and divided by the slope.[26] The calculated LOD and LOQ were 11.8 μg per filter and 39.2 μg per filter, respectively. Six of 59 samples analyzed in the analysis were below the LOD; 21 of 59 samples were between the LOD and the LOQ; 32 samples were above the LOQ.

Analysis of the Ti standards indicated that the internal instrument calibration was reliable based on the slope, intercept, and Pearson correlation coefficient from an orthogonal regression (Fig. 1). For this reason, measured readings instead of detector counts were used for all subsequent modeling efforts. The measured readings were slightly lower than the reported standard values (slope = 0.981).

The measurements at different locations on the filters were tested for normality using the Wilks Shapiro test; all positions had a non-normal distribution of measurements ($p < 0.05$). Natural log transformation did not yield a normal distribution; therefore, a Wilcoxon signed-rank test, the non-parametric equivalent of a *t*-test, was employed to compare the measurements between each pair of positions. The center measurement was different from all other positions ($p < 0.01$) confirming the non-uniform deposition expected from closed-face cassette sampling. The top, bottom, right, and left measurement sites were not different from each other ($p > 0.93$) indicating measurement uniformity (*i.e.* radial symmetry) around the perimeter of the filter.

An orthogonal regression was performed to compare the five- and two-point models to the gravimetric filter loadings using all 59 samples (Fig. 2). Slopes, intercepts, and Pearson correlation coefficients are virtually identical. Similar regression results were observed when only data above the LOQ were analyzed (data not shown). Multiple linear regression models show virtually equivalent results for five- *versus* two-point models as shown by percent recoveries (Fig. 2). An overestimation of 4% is observed from the regression slope. The two-point model was chosen as it is faster and easier to perform in the field. For the two-point model: for values less than the LOD (11.8 μg per filter), percent recoveries are less than 50%; between the LOD and the LOQ (39.3 μg per filter), percent recoveries ranged

Author Manuscript Author Manuscript Author Manuscript Author Manuscript

from 8 to 84%; for values greater than the LOQ, percent recoveries were greater than 70%. Only two measurements were over-predicted by more than 10%.

## LIBS

For the LIBS analysis, the 10 pieces cut from each of the 14 samples were each analyzed with a single shot. Atomic Ti emission was monitored at 264.6 and 336.1 nm, and atomic carbon emission, from the polycarbonate filter material, was monitored at 247.9 and 387.6 nm and used as an internal standard to reduce the effect of shot to shot variation. The 336.1 nm Ti transition occurs to the ground electronic state and is therefore susceptible to signal saturation at high sample loading conditions due to self-absorption. However, the 264.6 nm emission occurs from singly ionized Ti atoms to a non-ground state energy level, making it less likely to experience saturation. Signal saturation for the 336.1 nm emission and the non-saturating 264.6 nm emission are shown in Fig. 3.

In this study, the upper end of the linear dynamic range for the 264.6 nm Ti emission was limited by the sample preparation method to a loading of 252 μg per filter. At loadings near 500 μg per filter (*e.g.*, sample 69), the $TiO_2$ deposited on the PCTE filter cracked and peeled away from the surface when cutting the filter into pieces. Two possible solutions that may extend the dynamic range for LIBS measurements include: (1) collecting multiple filter samples of equal sample loading simultaneously, where each sample gets only one LIBS shot or (2) collecting the aerosol sample on a filter that entraps the material (*e.g.*, glass fiber filter), making the sample less likely to be disrupted when making multiple laser shots on a single filter. These solutions will be explored in a later study.

For LIBS measurements, the LOD was calculated as three times the standard deviation of the background divided by the slope of the calibration curve. The LOD's for the 264.6 and 336.1 nm emission peaks are 2.7 and 0.032 μg per filter, respectively. The LOQ's are 9.0 and 0.11 μg per filter, respectively. These results indicate that a two-peak analysis method is beneficial for LIBS measurements of titanium. At loadings below approximately 100 μg Ti per filter, both the 336.1 and 264.6 nm Ti emission lines were linear with loading (Fig. 3), but the 336.1 nm line provided a factor of 100 better LOD than the 264.6 nm emission line. At loadings above 100 μg Ti per filter, the 264.6 nm emission extends the linear dynamic range to at least 252 μg Ti per filter (Fig. 4). The actual upper bound of the dynamic range will be determined in a later study.

Using the calibration curves from Fig. 4, predicted Ti mass loadings of the fourteen samples were calculated and compared to the gravimetric analysis (Fig. 5). An overestimation of 2% is observed from the regression slope. For samples below 100 μg Ti per filter the 336.1 nm emission line calibration was used. For samples above 100 μg Ti per filter the calibration curve using the 264.6 nm emission line was used.

## FTIR

Preliminary analyses of $TiO_2$ on filter samples were conducted using all three FTIR methods (transmission, DR, ATR), in order to evaluate which method would be most capable of predicting the mass of $TiO_2$ on the samples. Potential interference from the filter material

Author Manuscript Author Manuscript Author Manuscript Author Manuscript

was first assessed. It was observed that in the region of interest (800–470 $cm^{-1}$) the spectra from all three methods contained peaks representing significant potential for interference, suggesting that the use of PCTE filters poses a challenge for the effective quantification of deposited $TiO_2$ material.

A total of 39 samples were analyzed using the three FTIR methods. Correlations to the gravimetric data (Fig. 6) indicate that the transmission method is more dependable than ATR or DR. This observation is likely because the transmitted signal is not affected as strongly by the variability in the interaction between the beam and the filter material since the beam repeatedly interacts with the same amount of filter material. This variability was especially noticeable at low filter loadings, where the transmission measurements display less variability around the trend line. The transmission method therefore produced a better correlation between peak areas and the mass of $TiO_2$ on the samples, as compared to ATR or DR. Results of the preliminary tests indicated that ATR is limited to loadings less than about 200 μg Ti per filter. It also had the downsides of variable interference from the PCTE filter and that it required the sample to be pressed against the ATR crystal, rendering it useless for most types of further analyses. The DR method, while it is not subject to the reduced signal for heavily loaded samples and is placed lightly onto the planar surface for analysis, is still hindered by variability in PCTE filter interference. The transmission method therefore proved to be the most amenable method for this filter type, especially since a robust field method would likely require subtraction of the filter contribution, which is only plausible for the transmission method due to the reasonably consistent contribution from the PCTE filter.

Using the equation of the calibration curve for transmission (Fig. 6c), a second sample set was analyzed and the raw FTIR data was transposed into estimates of filter loading for each sample (Fig. 7). While the method association is somewhat linear, the accuracy of prediction is lower ($R^2$ = 0.831) than for XRF or LIBS, and the data varies considerably from the line of best fit, suggesting large standard deviations. The lack of accuracy and repeatability in quantifying the $TiO_2$ is a result of the substantial variability in measured peak areas, stemming from the fact that $TiO_2$ absorbs IR radiation over a fairly wide range of wavelengths, making it more susceptible to interferences. It is also a function of the interference from the PCTE filters in the analytical region, which could possibly be reduced or eliminated in the future by choice of a different filter material.

The actual LOD and LOQ were calculated using a similar approach as for the other methods and were 108.4 μg per filter and 361.0 μg per filter, respectively. Of the 25 samples remaining in the analysis, 11 were below the LOD, 12 were between the LOD and the LOQ, and two were above the LOQ.

## Conclusions

With an eye toward field-portable analysis of ultrafine $TiO_2$ dust, three potential methods were evaluated for quantification of $TiO_2$ samples collected on PCTE filters (Table 2). XRF was very suitable for this application, since it produced accurate results with a wide linear dynamic range, *i.e.*, from 39.2 (LOQ) to 578 μg Ti per filter. LIBS was also suitable, especially for lightly loaded samples, since it has a very low LOQ of 0.11–9.0 μg Ti per

Author Manuscript Author Manuscript Author Manuscript Author Manuscript

filter, which depended on which Ti emission line was used for analysis. However, due to friability of deposited material from the PCTE filter, an alternate sample preparation method would need to be used for samples above about 250 μg Ti per filter. While both LIBS and XRF have the potential downside of susceptibility to interference by non-$TiO_2$ sources of Ti, it is generally assumed that the occurrence of such confounders is highly unlikely in workplace atmospheres. FTIR analyses were deemed undependable due to the broad-band absorption characteristics of $TiO_2$ and to excessive interference due to the PCTE filter itself.

As evidenced by the results of Koivisto *et al*. (2012), there is a critical need for rapid and specific analysis of Ti mass exposures among pigment and nanoscale powder workers.[8] The ability to quantify Ti mass on filter samples at the end of a work shift would provide exposure assessors with a powerful tool for characterizing and managing exposures. Based on the respirable REL of 0.3 mg $m^{-3}$ and a flow rate of 3 LPM over an 8 h shift, Ti mass loading at the REL would be 302 μg and could easily be measured by XRF, while that loading may require an alternate sample preparation method for analysis by LIBS. Measurement variability of FTIR for $TiO_2$ on PCTE filters due to analytical interferences may preclude the use of that technique for this particular sampling strategy; however, alternate filter materials could be investigated and may prove more promising. XRF is less expensive than the other two methods considered and is portable and non-destructive, making it an appropriate choice for field-based measurements of filter samples at end-of-shift. It has been shown to produce more repeatable analyses than LIBS under similar conditions,[27] and since sample integrity is maintained, it allows for further analyses of samples (*e.g*. surface area,[10] particle morphology, and confirmation of mass loadings). In addition, more timely exposure characterization is produced by XRF in comparison to traditional shipment to a laboratory and analysis by ICP-AES. Based on the current work, XRF can be expected to accurately and reproducibly measure Ti content on PCTE filter samples, and was therefore chosen over FTIR and LIBS as the best method for this filter type and form of material.

Our results are in agreement with previous work which demonstrated that XRF may be used for the qualitative, semi-quantitative, or quantitative determination of Ti[28,29] as well as other elements30–34 in various matrices. As with any analytical technique, interferences and errors introduced by sampling or the sampling environment must be considered. For example, filters collected for these experiments contained no matrix interferences, which may be seen in real-world samples. While this work established the efficacy of using field portable techniques for end-of-shift mass measurements, a need remains for further research to validate these techniques as a viable tool for industrial hygienists.

## Reference

1. Donaldson K, Stone V, Gilmour PS, Brown DM, MacNee W. Philos. Trans. R. Soc., A. 2000; 358:2741–2749.
2. Ferin J, Oberdorster G, Penney DP. Am. J. Respir. Cell Mol. Biol. 1992; 6:535–542. [PubMed: 1581076]
3. NIOSH. [accessed 11 February 2013] Current Intelligence Bulletin 63: Occupational Exposure to Titanium Dioxide. http://www.cdc.gov/niosh/docs/2011-160/pdfs/2011-160.pdf

Author Manuscript Author Manuscript Author Manuscript Author Manuscript


4. ACGIH. 2011 Threshold Limit Values for Chemical Substances and Physical Agents & Biological Exposure Indices; American Conference of Governmental Industrial Hygienists; Cincinnati, OH. 2011.
5. Fryzek JP, Chadda B, Marano D, White K, Schweitzer S, McLaughlin JK, Blot WJ. J. Occup. Environ. Med. 2003; 45:400–409. [PubMed: 12708144]
6. Curwin B, Bertke S. J. Occup. Environ. Hyg. 2011; 8:580–587. [PubMed: 21936697]
7. Huang C-H, Tai C-Y, Tsai C-J, Chen C-W, Chang C-P, Shih T-S. J. Environ. Sci. Health, Part A: Toxic/Hazard. Subst. Environ. Eng. 2010; 45:1227–1233.
8. Koivisto A, Lyyränen J, Auvinen A, Vanhala E, Hämeri K, Tuomi T, Jokiniemi J. Inhalation Toxicol. 2012; 24:839–849.
9. Chen, B.; Frazer, D.; Stone, S.; Schwegler-Berry, D.; Cumpston, J.; McKinney, W.; Lindsley, W.; Frazer, A.; Donlin, M.; Vandestouwe, K.; Castranova, V. Proceedings of the Seventh International Aerosol Conference; St. Paul, MN; 2006.
10. LeBouf RF, Stefaniak AB, Chen BT, Frazer DG, Virji MA. Nanotoxicology. 2011; 5:687–699. [PubMed: 21261457]
11. Morley JC, Clark CS, Deddens JA, Ashley K, Roda S. Appl. Occup. Environ. Hyg. 1999; 14:306–316. [PubMed: 10446483]
12. Skoog, DA.; Holler, FJ.; Crouch, SR. Principles of Instrumental Analysis. 6th. Belmont, CA: Thomson Brooks/Cole; 2007.
13. Cremers, D.; Radziemski, L. Handbook of Laser-Induced Breakdown Spectroscopy. West Sussex, England: John Wiley & Sons; 2006.
14. Cremers D, Radziemski L. Appl. Spectrosc. 1985; 39:57–63.
15. Neuhauser R, Panne U, Niessner R. Anal. Chim. Acta. 1999; 392:47–54.
16. Panne U, Neuhauser R, Theisen M, Fink H, Niessner R. Spectrochim. Acta, Part B. 2001; 56:839–850.
17. Stipe C, Miller A, Brown J, Guevara E, Cauda E. Appl. Spectrosc. 2012; 66:1286–1293. [PubMed: 23146184]
18. Griffiths, PR.; de Haseth, JA., editors. Fourier Transform Infrared Spectrometry. New York: John Wiley & Sons; 1986.
19. Alperti, NL.; Keiser, WE.; Szymanski, HA. IR-theory and practice of infrared spectroscopy. Plenum/Rosetta: 1973.
20. Sui R, Rizkalla A, Charpentier P. J. Phys. Chem. B. 2006; 110:16212–16218. [PubMed: 16913745]
21. Miller A, Drake P, Murphy N, Noll J, Volkwein J. J. Environ. Monit. 2012; 14:48–55. [PubMed: 22130611]
22. Schecht, PC.; O'Connor, PF., editors. NIOSH. NIOSH Manual of Analytical Methods (NMAM). 4th. Washington, D.C.: Centers for Disease Control and Prevention, NIOSH; 2003. Pub. no. 94-113
23. Tuchman, D. US Department of Interior (BOM). Washington, DC: 1992. p. 1-17.
24. Scarel G, Aita C, Tanaka H, Hisano K. J. Non-Cryst. Solids. 2002; 303:50–53.
25. Hill, BK. M. S. Thesis. University of Iowa: 2012.
26. Kennedy, ER.; Fischbach, TJ.; Song, R.; Eller, PM.; Shulman, SA. Guidelines for Air Sampling and Analytical Method Development and Evaluation. Cincinatti: National Institute of Occupational Safety and Health; 1995. Pub no. 95-117
27. Pouzar M, Průšová M, Černohorský T, Wiener J, Kratochvil T. J. Appl. Spectrosc. 2011; 78:673–679.
28. Suzuki EM, McDermot MX. J. Forensic Sci. 2006; 51:532–547. [PubMed: 16696700]
29. Nishiwaki Y, Watanabe S, Shimoda O, Saito Y, Nakanishi T, Terada Y, Ninomiya T, Nakai I. J. Forensic Sci. 2009; 54:564–570. [PubMed: 19302400]
30. Siyanbola WO, Fasasi AY, Funtua II, Afolabi OM, Adesiyan TA. Nucl. Instrum. Methods Phys. Res., Sect. B. 2004; 215:240–245.

Author Manuscript Author Manuscript Author Manuscript Author Manuscript

31. Pappalardo L, de Sanoit J, Marchetta C, Pappalardo G, Romano FP. X-Ray Spectrom. 2007; 36:310–315.
32. Gazquez MJ, Bolivar JP, Garcia-Tenorio R, Vaca F. J. Hazard. Mater. 2009; 166:1429–1440. [PubMed: 19167156]
33. Sokaras D, Karydas AG, Oikonomou A, Zacharias N, Beltsios K, Kantarelou V. Anal. Bioanal. Chem. 2009; 395:2199–2209. [PubMed: 19821114]
34. Laohaudomchok W, Calvallari J, Fang S, Lin X, Herrick R, Christiani D, Weisskopf M. J. Occup. Environ. Hyg. 2012; 7:456–465. [PubMed: 20526948]

Author Manuscript Author Manuscript Author Manuscript Author Manuscript

## Environmental impact

A need exists for rapid and selective characterization of exposures to ultrafine titanium dioxide in workplace atmospheres. Field portable measurements of titanium dioxide may provide more timely assessment of exposure than traditional techniques such as gravimetric or inductively coupled plasma atomic emission spectrometry. This study describes the comparison of field portable measurements of filters loaded with ultrafine titanium dioxide. The analysis techniques include X-ray fluorescence, laser-induced breakdown spectroscopy, and Fourier-transform infrared spectroscopy. Since non-destructive techniques such as X-ray fluorescence maintain sample integrity, further analyses may be performed to confirm mass or holistically characterize the sample in terms of morphology and surface area.

Author Manuscript Author Manuscript Author Manuscript Author Manuscript

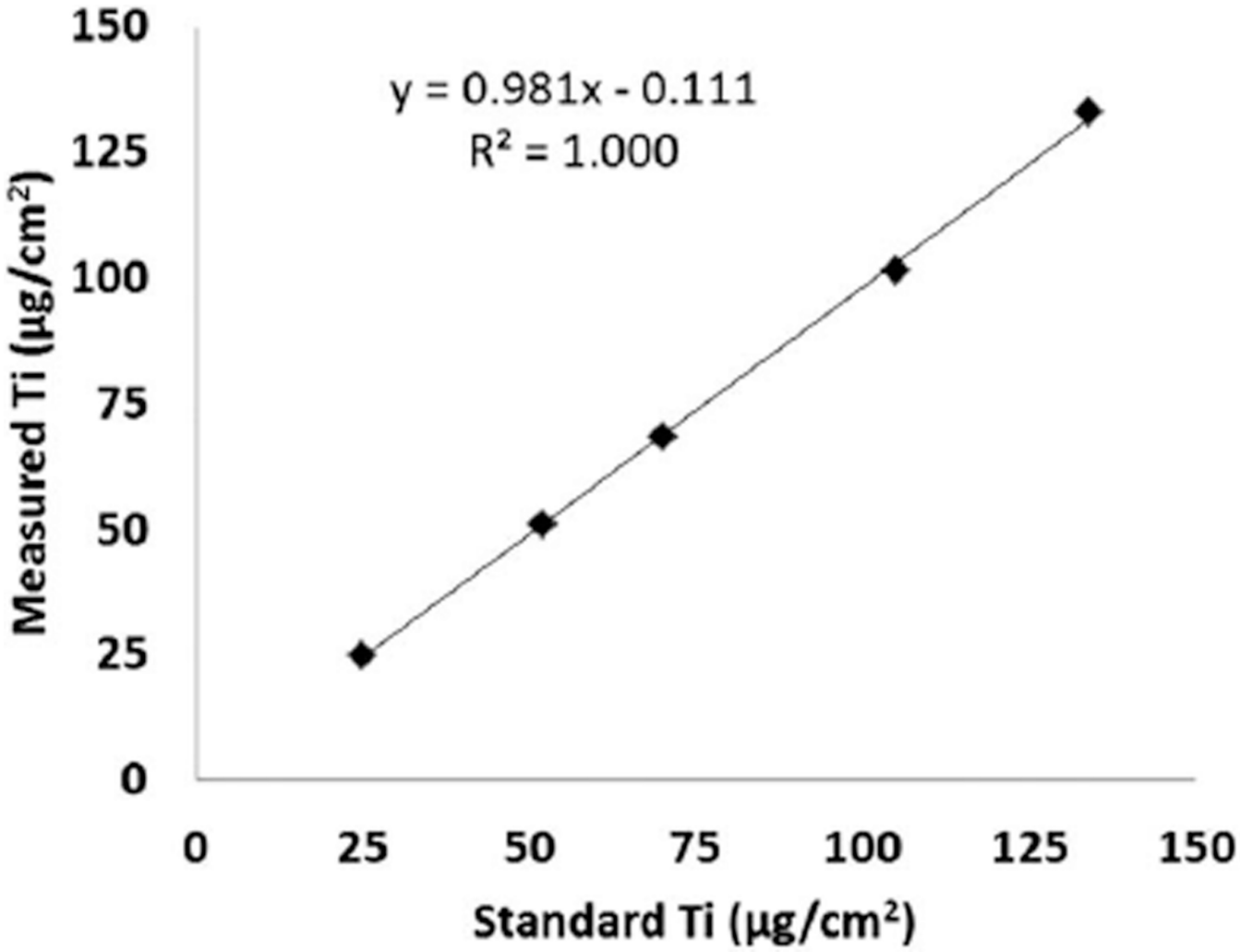


**Fig. 1.**
Titanium standard calibration curve.

Author Manuscript Author Manuscript Author Manuscript Author Manuscript

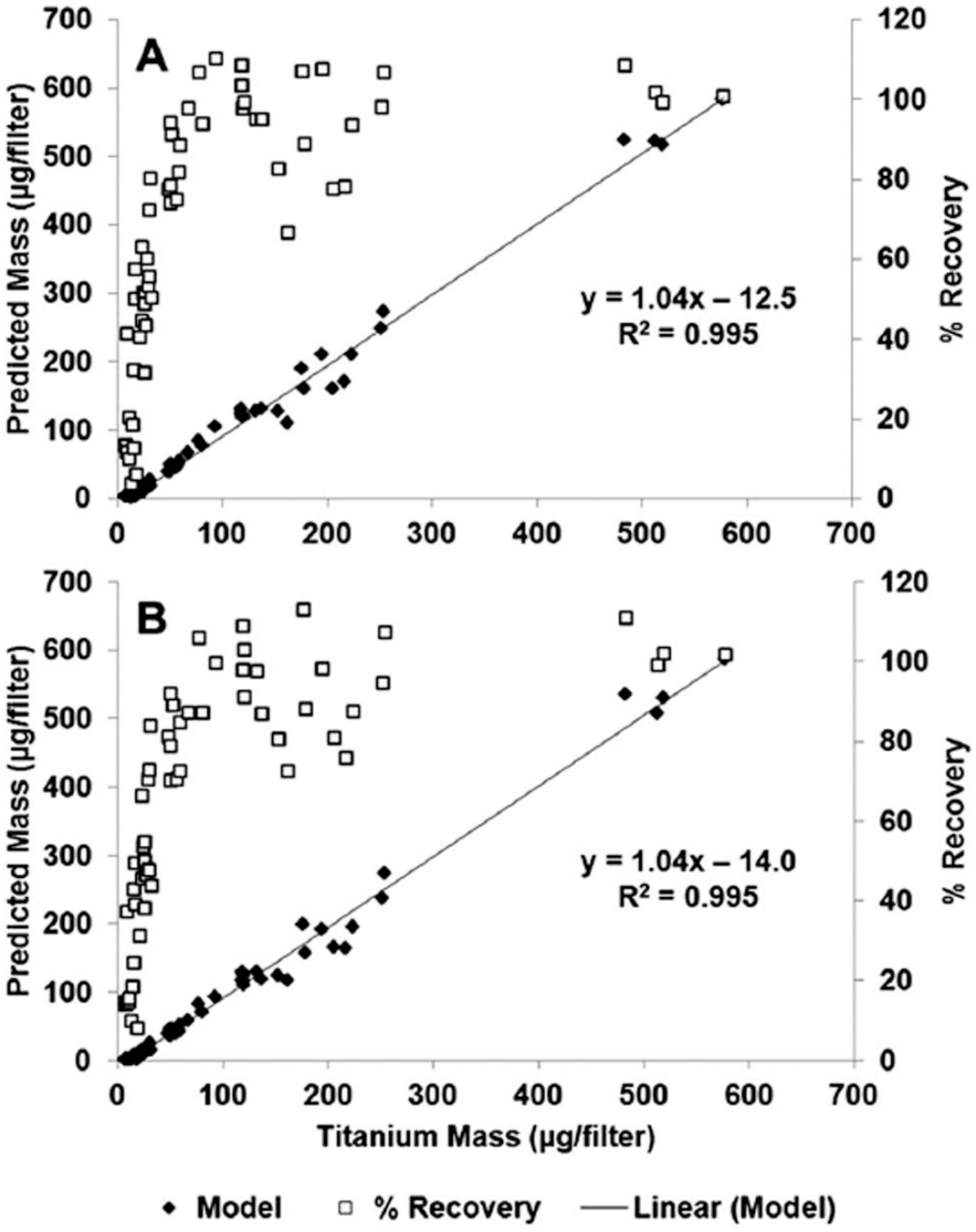


**Fig. 2.**

Orthogonal regression of filter titanium mass loadings and percent recoveries based on (A) five-point model and (B) two-point model.

Author Manuscript Author Manuscript Author Manuscript Author Manuscript

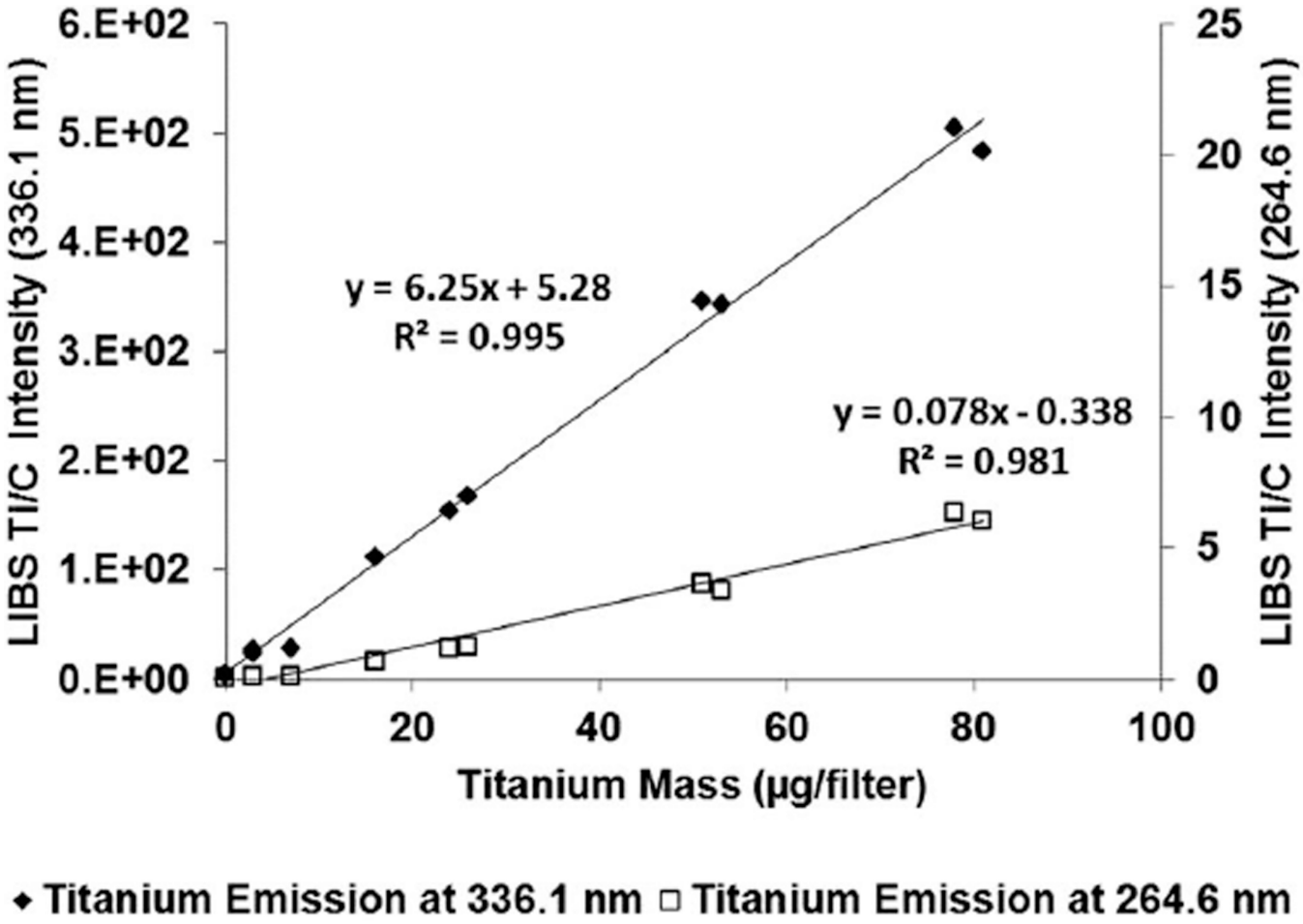


**Fig. 3.**

Titanium LIBS signal *versus* filter mass loading for loadings below 80 µg per filter. The "filled" diamonds are for titanium emission at 336.1 nm and "open" squares are for emission at 264.6 nm. At low loadings, the calibration curves for both the 336.1 and 264.6 nm emission peaks are linear.

Author Manuscript Author Manuscript Author Manuscript Author Manuscript

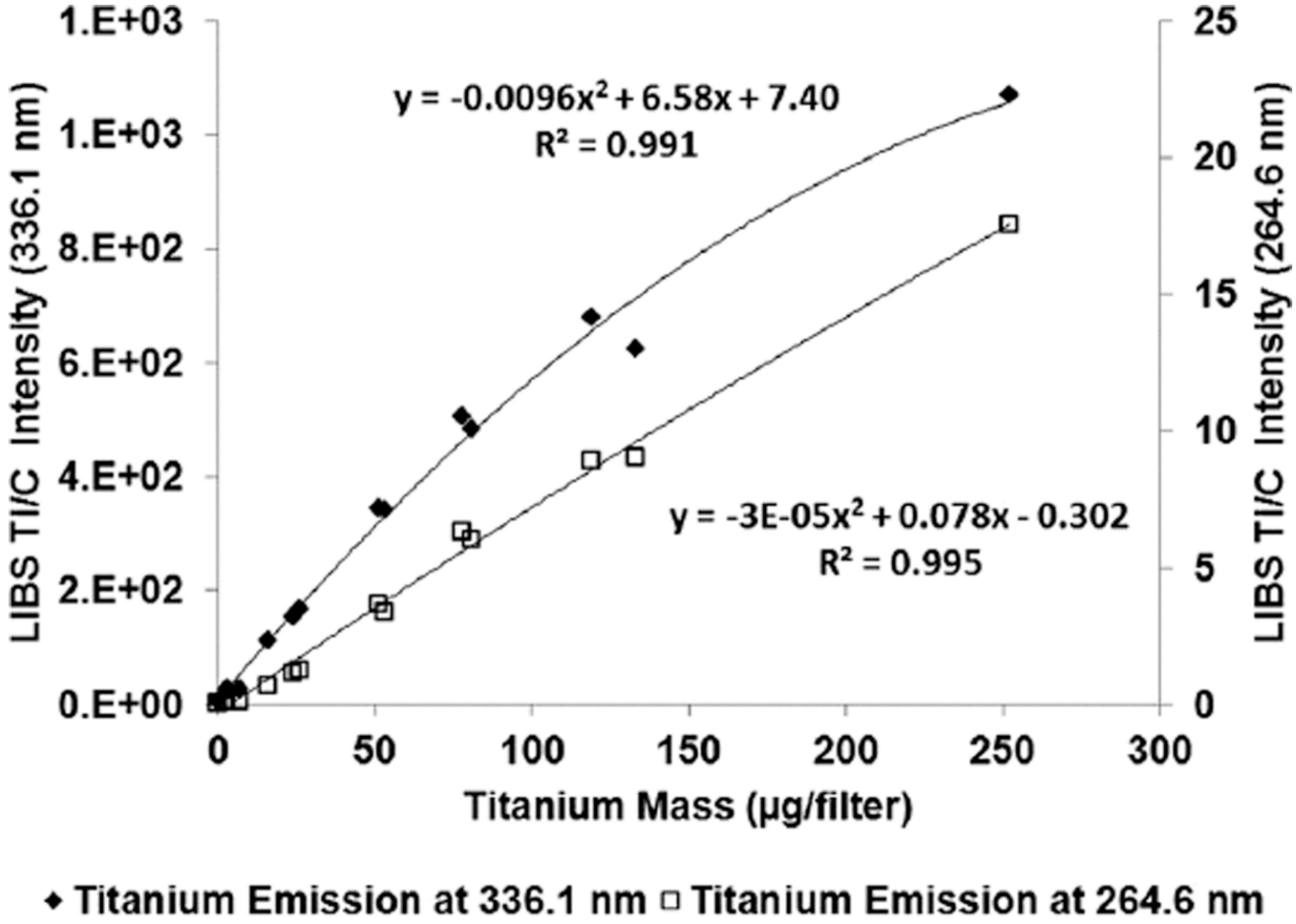


**Fig. 4.**

Titanium LIBS signal *versus* filter mass loading. The “filled” diamonds are for titanium emission at 336.1 nm and “open” squares are for emission at 264.6 nm.

Author Manuscript Author Manuscript Author Manuscript Author Manuscript

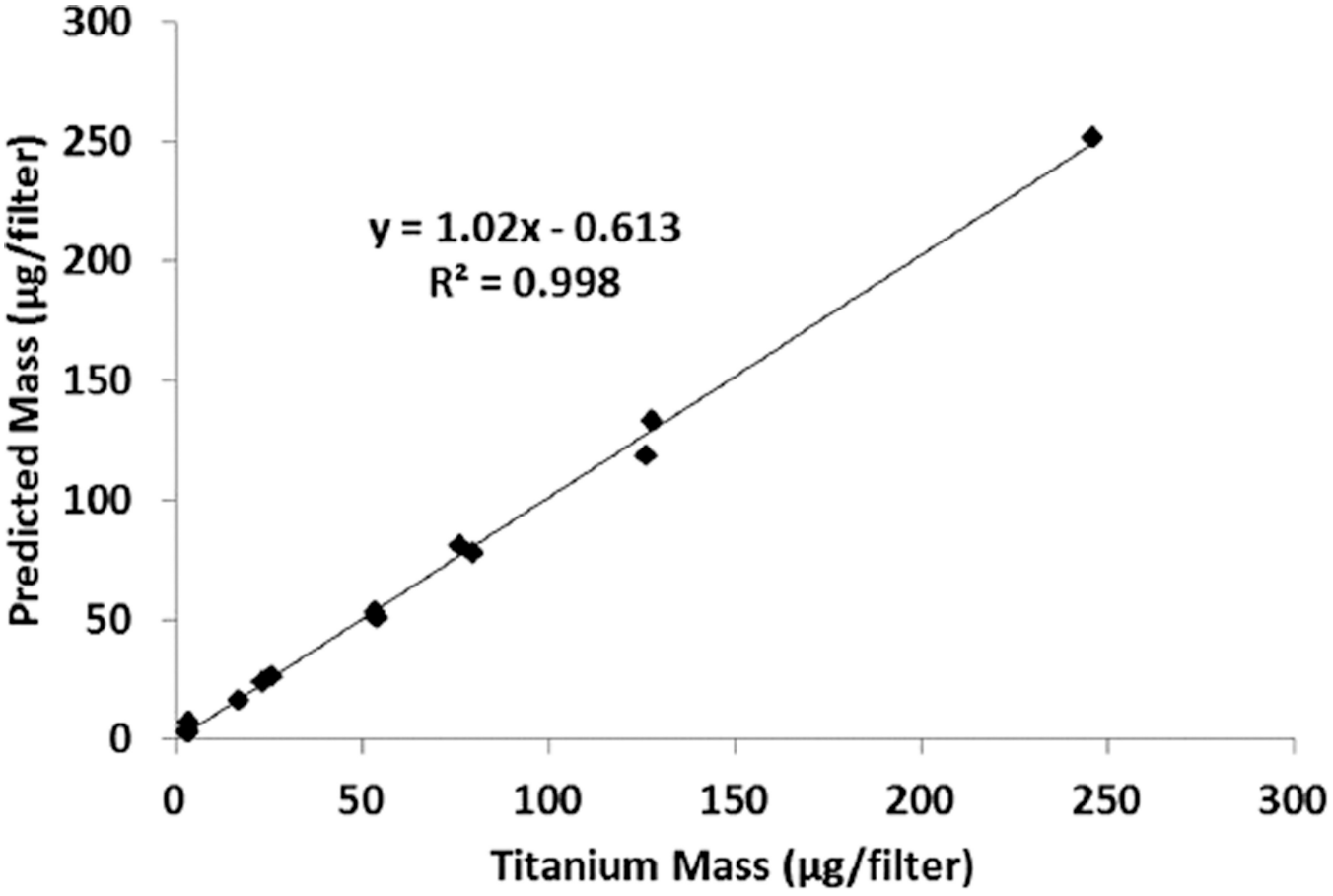


**Fig. 5.**
Correlation between LIBS data and the (known) gravimetric data.

Author Manuscript Author Manuscript Author Manuscript Author Manuscript

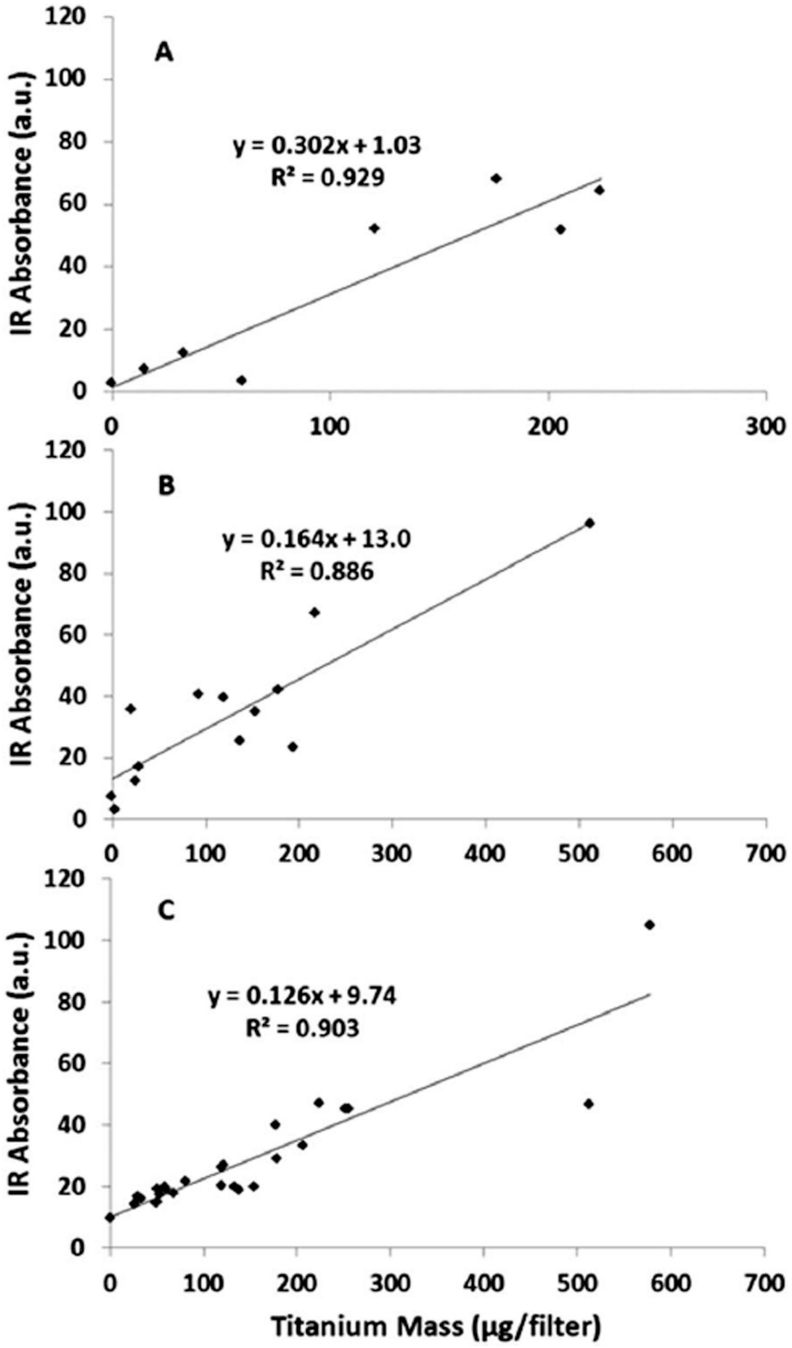


**Fig. 6.**

Calibration curves for the integrated peak areas (800–470 $cm^{-1}$) *versus* titanium mass loading for a subset of the filter samples using FTIR in the: (a) ATR, (b) DR, and (c) transmission modes.

Author Manuscript Author Manuscript Author Manuscript Author Manuscript

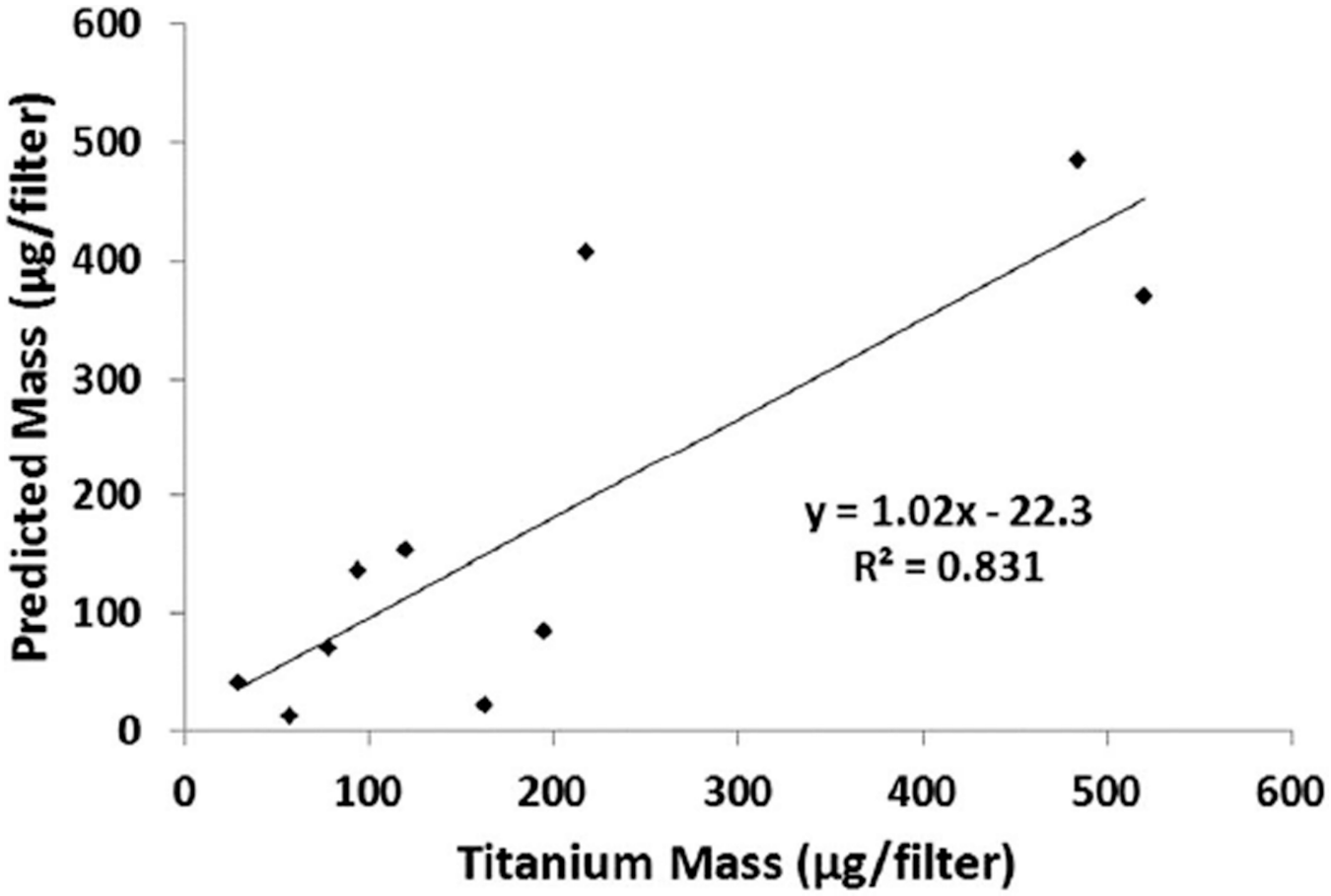


**Fig. 7.**
Correlation between FTIR data and the (known) gravimetric data for those samples not used in generating the calibration curve.

Author Manuscript Author Manuscript Author Manuscript Author Manuscript



*Environ Sci Process Impacts*. Author manuscript; available in PMC 2016 January 11.

**Table 1**

Identification of samples and associated elemental titanium mass loadings

| Sample # | Ti mass (μg) | Sample # | Ti mass (μg) | Sample # | Ti mass (μg) |
|---|---|---|---|---|---|
| 1 | 3 | 26 | 17 | 51 | 51 |
| 2 | 4 | 27 | 18 | 52 | 60 |
| 3 | 3 | 28 | 32 | 53 | 68 |
| 4 | 3 | 29 | 4 | 54 | 94 |
| 5 | 3 | 30 | 5 | 55 | 78 |
| 6 | 3 | 31 | 3 | 56 | 81 |
| 7 | 3 | 32 | 3 | 57 | 120 |
| 8 | 7 | 33 | 11 | 58 | 121 |
| 9 | 6 | 34 | 15 | 59 | 119 |
| 10 | 7 | 35 | 16 | 60 | 119 |
| 11 | 6 | 36 | 16 | 61 | 163 |
| 12 | 5 | 37 | 30 | 62 | 177 |
| 13 | 12 | 38 | 29 | 63 | 133 |
| 14 | 19 | 39 | 26 | 64 | 138 |
| 15 | 9 | 40 | 33 | 65 | 224 |
| 16 | 14 | 41 | 51 | 66 | 252 |
| 17 | 24 | 42 | 51 | 67 | 195 |
| 18 | 26 | 43 | 57 | 68 | 255 |
| 19 | 24 | 44 | 59 | 69 | 520 |
| 20 | 25 | 45 | 179 | 70 | 578 |
| 21 | 31 | 46 | 154 | 71 | 513 |
| 22 | 27 | 47 | 218 | 72 | 484 |
| 23 | 29 | 48 | 206 | | |
| 24 | 26 | 49 | 49 | | |
| 25 | 21 | 50 | 53 | | |

Author Manuscript

Author Manuscript

Author Manuscript

Author Manuscript

**Table 2**

Performance of three portable methods for measuring $TiO_2$ on filter samples

| Method | LOD (μg Ti per filter) | LOQ (μg Ti per filter) | Dynamic range (μg Ti per filter) |
|---|---|---|---|
| XRF | 11.8 | 39.3 | 11.8–578 (max) |
| LIBS (264) | 2.7 | 9.0 | 2.7–252 |
| LIBS (336) | 0.032 | 0.11 | 0.032–100 |
| FTIR | 108.4 | 361 | 108.4–578 (max) |